Hydrogen Bonding and Size Effects of Cations on the Coordination Geometry of Metal Ions. Tetrahalocobaltates(II) of the *N*-Ethyl-, 2-Ethyl-, and 4-Benzylpiperidine Cations. Crystal and Molecular Structure of Bis(4-benzylpiperidinium) Tetrachlorocobaltate(II)

L. ANTOLINI,[1a] G. MARCOTRIGIANO,[1b] L. MENABUE,[1a] and G. C. PELLACANI*[1a]

Some compounds of the type (LH)$_2$CoX$_4$ (LH = *N*-ethyl-, 2-ethyl-, and 4-benzylpiperidinium cations; X = Cl, Br, I) were prepared and characterized by means of magnetic moments and X-ray powder, electronic, and infrared spectra. For one of them, bis(4-benzylpiperidinium) tetrachlorocobaltate(II), the crystal structure was determined by three-dimensional X-ray diffraction. The substance crystallizes in space group $P2_1$ with lattice constants $a = 13.469$ (3) Å, $b = 8.416$ (2) Å, $c = 12.169$ (3) Å, $\beta = 97.54$ (5)°, and $Z = 2$. The intensity data were collected with a Philips PW 1100 automatic four-circle diffractometer using Mo Kα radiation. The structure was solved by three-dimensional Patterson and Fourier methods, and parameters were refined by least-squares calculations to a conventional R factor of 4.8% for 1209 independent reflections [$I > 3\sigma(I)$]. The structure consists of discrete CoCl$_4^{2-}$ and 4-benzylpiperidinium ions; the slightly distorted tetrahedral anions are bridged by hydrogen bonds involving the NH$_2$ groups of the cations. The magnetic moments and electronic and far-IR spectra of the complexes indicate distorted tetrahedral environments in the 4-benzylpiperidinium complexes greater than those in the *N*-ethyl- and 2-ethylpiperidinium complexes. The far-IR spectrum of the bis(4-benzylpiperidinium) tetrachlorocobaltate(II) complex is interpreted on the basis of a C_2 symmetry.

Introduction

Our interest in the conditions which have a determining influence on the geometry of the halo complexes derives from their great ease in assuming various geometries. In our previous investigations on halometalates (M = Cu(II),[2,3] Sn(IV), Sb(III), and Bi(III)[4]) the geometries of the complexes were found to depend on the crystal packing forces and hydrogen bonding ability of the countercations. In fact, cations having a great hydrogen bonding ability stabilize strongly distorted tetrahedral structures for the tetrachlorocuprates[2,3] and square-pyramidal structures for the pentahalometalates (M = Sb(III) and Bi(III)).[4]

In this paper we have considered the complexes formed between the *N*-ethyl-, 2-ethyl-, and 4-benzylpiperidinium cations (hereafter abbreviated *N*-EtpipdH, 2-EtpipdH, and 4-BzpipdH, respectively) and the cobalt(II) halides. All synthesized compounds were characterized by means of spectral and magnetic properties, and for one of them, the electronic and far-IR spectra of which indicate the presence of distortion from tetrahedral symmetry greater than that of the other halocobaltates(II) considered in this work, the crystal structure was also determined.

Experimental Section

Preparation of the Hydrohalide Salts. All the hydrohalide salts were prepared by evaporating slowly and completely an aqueous amine solution neutralized with concentrated hydrogen halide. All the salts were recrystallized from ethanol and diethyl ether.

Preparation of the Complexes. (2-EtpipdH)$_3$CoCl$_5$ and (*N*-EtpipdH)$_2$CoX$_4$ (X = Cl, Br) complexes were prepared by adding diethyl ether to an ethanolic solution of CoX$_2$·6H$_2$O (1 mmol) and hydrohalide salt (2 mmol), and an oil was separated; when the oil was cooled for some hours at 4 °C, crystals precipitated.

(LH)$_2$CoX$_4$ (LH = 4-BzpipdH and X = Cl, Br; LH = 2-EtpipdH and X = Br) complexes were precipitated by cooling at 4 °C a solution containing CoX$_2$·6H$_2$O (1 mmol) and the corresponding hydrohalide salts (2 mmol) in methanol + ethanol (1:1).

The (4-BzpipdH)$_2$CoI$_4$ complex was obtained by adding to an aqueous solution containing 2CoCO$_3$·3Co(OH)$_2$·nH$_2$O and the amine an excess of concentrated hydrogen iodide until the solution became green. The solution was evaporated until a green compound was separated, which was recrystallized from ethanol.

All the other iodide derivatives were obtained by mixing the metal salt and the amine in ethanol, by adding concentrated hydrogen iodide until the solution became green, and by concentrating and allowing the solution to stand for some days at room temperature. The compounds separated were dried under vacuum on KOH.

Physical Measurements. The electronic spectra of the solid compounds were recorded as mull transmission spectra with a Shimadzu MPS 50L spectrophotometer. The infrared spectra of NaCl or KBr pellets (4000–250 cm^{-1}) and of Nujol mulls (400–60 cm^{-1}) were recorded with a Perkin-Elmer 180 spectrophotometer. The room-temperature magnetic moments were measured with the Gouy method by using HgCo(NCS)$_4$ as calibrant and correcting for diamagnetism with the appropriate Pascal constants and for the temperature-independent paramagnetism (TIP).[5] Differential scanning calorimetric analyses were performed with a Perkin-Elmer DSC-1 instrument.

Crystallographic Data Collection. The crystal selected for X-ray data collection had dimensions of 0.37 mm × 0.19 mm × 0.07 mm and was sealed in a glass capillary, since the crystals appeared to be slightly hygroscopic.

Data were collected at room temperature with a Philips PW1100 automatic four-circle diffractometer using graphite-monochromated Mo Kα radiation ($\lambda = 0.71069$ Å).

The unit cell parameters were determined by using the standard control program of the PW1100 system[6] with a randomly oriented crystal and derived from least-squares refinement of the setting angles of 25 strong high-angle reflections. Crystals are monoclinic: $a = 13.469$ (3), $b = 8.416$ (2), $c = 12.169$ (3) Å; $\beta = 97.54$ (5)°; $V = 1367.5$ Å^3.

Integrated intensities for $-h_{max} \leq h \leq h_{max}$ with k and $l \geq 0$ reflections and $3° < \theta < 23°$ were measured by using the ω–2θ scan method, a scan speed of 3.0° min^{-1}, a scan width of 1.20°, and two background counts of 10 s at each end of the scan. Throughout data collection, two intense reflections were monitored at 120-reflection intervals; intensities of these standards showed no significant variations.

A total of 2064 independent reflections were measured, and the recorded intensities and $\sigma(I)$ values evaluated as (peak counts + total background counts)$^{1/2}$ were corrected for Lorentz and polarization factors, but not for absorption; 1209 reflections for which $I > 3.0\sigma(I)$ were denoted observed and were used in the structure analysis.

Inspection of intensities revealed the systematic absences 0*k*0, *k* = 2*n* + 1. This condition is consistent with space groups $P2_1$ (C_2^2, No. 4) and $P2_1/m$ (C_{2h}^2, No. 11). As shown by the subsequent solution of the structure, $P2_1$ is the correct space group.

The measured density, determined by flotation on CHCl$_3$–ClC-H$_2$CH$_2$Cl solutions, was 1.33 g/cm^3; the calculated density is 1.343 g/cm^3 for 2 formula units per cell.

Solution and Refinement of Structure. Scattering factors for Co^{2+} and Cl$^-$ ions, including real and imaginary terms of anomalous dispersion, and for N, C, and H atoms were taken from ref 7. The function minimized during least-squares refinements was $\sum w(|F_o| - |F_c|)^2$; discrepancy indices used below are $R = (\sum ||F_o| - |F_c||)/\sum|F_o|$ and $R_w = [\sum w(|F_o| - |F_c|)^2/\sum w|F_o|^2]^{1/2}$, where w is the weighting factor.

Table I. Analytical Results

|	color	%C calcd	%C found	%H calcd	%H found	%N calcd	%N found	%X calcd	%X found	mp, °C
(N-EtpipdH)$_2$CoCl$_4$	blue	39.15	39.20	7.51	7.32	6.53	5.86	33.05	33.11	105–109
(N-EtpipdH)$_2$CoBr$_4$	blue	27.68	27.49	5.31	5.23	4.61	4.69	52.67	52.23	131–135
(N-EtpipdH)$_2$CoI$_4$	green	21.19	21.47	3.81	4.18	3.53	3.41	64.03	64.90	158–162
(2-EtpipdH)$_3$CoCl$_5$	blue	43.55	43.47	8.36	8.57	7.26	7.21	30.63	30.45	93–97
(2-EtpipdH)$_2$CoBr$_4$	blue	27.68	27.99	5.31	5.56	4.61	4.69	52.67	52.55	140–144
(2-EtpipdH)$_2$CoI$_4$	green	21.19	22.20	3.81	4.30	3.53	3.59	64.03	64.20	170–174
(4-BzpipdH)$_2$CoCl$_4$	blue	52.07	52.09	6.56	6.79	5.06	5.09	25.64	25.63	135–139
(4-BzpipdH)$_2$CoBr$_4$	blue	39.51	39.21	4.97	4.95	3.84	3.69	43.85	44.15	169–174
(4-BzpipdH)$_2$CoI$_4$	green	31.34	31.54	3.95	4.14	3.05	2.95	55.24	55.58	193–197
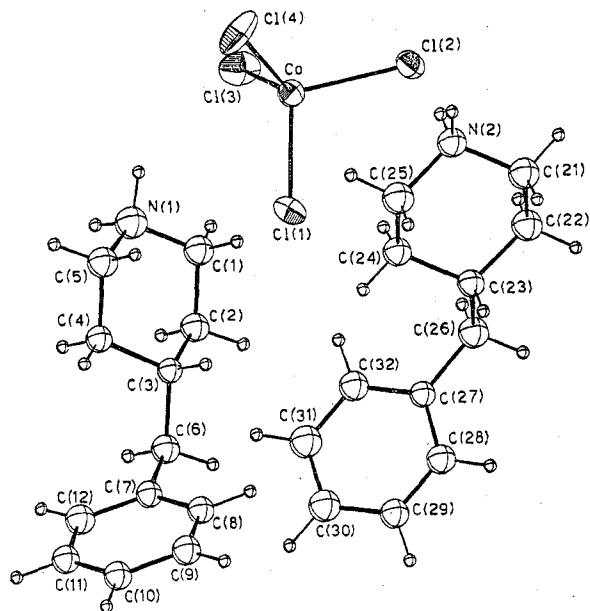
Figure 1. ORTEP drawing of the (4-BzpipdH)$_2$CoCl$_4$ molecule showing the labeling scheme and thermal motion ellipsoids (40%) for non-hydrogen atoms. The spheres corresponding to the hydrogen atoms are on an arbitrary scale.

A three-dimensional Patterson synthesis[8] revealed the approximate location of the tetrahedral CoCl$_4^{2-}$ ion and also indicated the space group $P2_1$ as the correct one; the space group $P2_1m$ requires the Co and two Cl atoms to lie on the mirror plane at $y = {}^1/_4$. The origin of the unit cell was arbitrarily defined by assigning a value of 0.25 to the y coordinate of the Co atom.

A Fourier synthesis, phased by contributions of Co and Cl atoms, revealed the locations of all N and C atoms. Block-diagonal least-squares refinement of atomic positional and isotropic thermal parameters, using unit weights, led to convergence at $R = 0.082$ and $R_w = 0.098$.

Final full-matrix least-squares refinement, including 36 fixed H atoms at their calculated positions (C–H and N–H = 1.00 Å) with an isotropic thermal parameter 1.0 Å^2 greater than that of the atom to which they are bonded and including anisotropic motion on Co and Cl atoms, lowered R to 0.048 and R_w to 0.062. This refinement was

performed with Cruickshank's weighting scheme $w = (2.0 + 0.07|F_o| + 0.002|F_o|^2)^{-1}$, to remove an F_o and $(\sin \theta)/\lambda$ dependence in the quantity $w(|F_o| - |F_c|)^2$, observed with $w = 1/\sigma^2(F)$ and with unit weights.

In the final least-squares cycle the shifts in all parameters were less than 0.3 of an esd. The "goodness of fit", defined as $[\sum w(|F_o| - |F_c|)^2/(N_o - N_v)]^{1/2}$, where $N_o = 1209$ is the number of reflections and $N_v = 150$ is the number of parameters varied, was 0.815.

A final difference Fourier synthesis revealed no significant electron density, with no peak greater than 0.35 e Å^{-3}. Correction for secondary extinction was not deemed necessary.

An attempt to establish the absolute configuration through least-squares refinement of the structure of opposite polarity, by changing the sign of k for all reflection data, failed because convergence was reached at the same previous R and R_w values (0.048 and 0.062, respectively) with only small parameter shifts; all results are therefore reported in terms of the first model.

Analyses. Nitrogen, carbon, and hydrogen were analyzed by Mr. Giuseppe Pistoni using a Perkin-Elmer 240 elemental analyzer. The halogens were directly determined in aqueous solutions of the complexes with the Volhard method.

Results and Discussion

The analytical results are reported in Table I. All the compounds are crystalline, hygroscopic, and soluble in polar organic solvents. Differential scanning calorimetric analysis of the compounds indicates that they are pure and that no phase transitions are present. Final positional and thermal parameters are given in Table II.

Description of the Structure. A drawing of the structure, showing the labeling scheme, is given in Figure 1 and a drawing of the unit cell contents in Figure 2. The bond lengths are listed in Table III and bond angles in Table IV.

The structure consists of discrete CoCl$_4^{2-}$ and 4-BzpipdH$^+$ ions linked by hydrogen bonds.

The cobalt atom exhibits a slightly distorted tetrahedral coordination, as previously found on structural investigations of a number of compounds containing the tetrachlorocobaltate(II) ion, for several of which the range of bond distances and bond angles is reported in Table V.[9–14] The mean Co–Cl bond distance of 2.277 Å and the maximum difference of 0.059 Å on Co–Cl bond lengths and of 6.9° on Cl–Co–Cl bond angles agree with previously found values. The deviation from T_d symmetry is less marked on estimating the
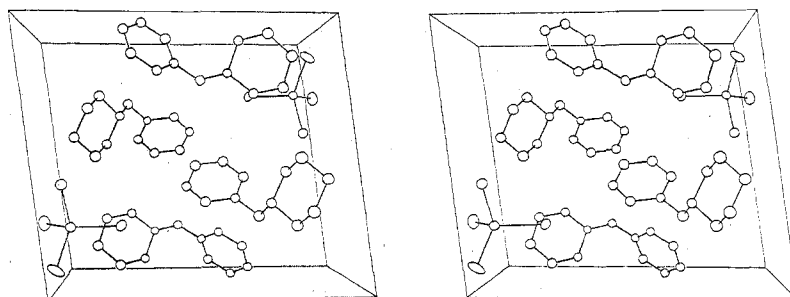

Figure 2. Stereoscopic view of the unit cell contents of (4-BzpipdH)$_2$CoCl$_4$ down the y axis. The origin is at the front upper left, with the x axis horizontal and the z axis vertical. The hydrogen atoms have been omitted for clarity.

Table II. Atomic Positional and Temperature Parameters for (4-BzpipdH)$_2$CoCl$_4$[a,b]

atom	x	y	z	B_{11}	B_{22}	B_{33}	B_{12}	B_{13}	B_{23}
Co	0.0763 (1)	0.2500	0.2401 (1)	3.65 (7)	3.17 (8)	3.73 (8)	−0.03 (8)	0.26 (6)	−0.27 (9)
Cl(1)	0.2368 (2)	0.3269 (5)	0.2407 (3)	4.41 (17)	4.53 (18)	5.09 (18)	−0.88 (15)	1.84 (14)	−0.03 (16)
Cl(2)	0.0767 (2)	0.1090 (5)	0.4032 (3)	4.50 (16)	4.00 (18)	4.14 (16)	−0.78 (15)	0.75 (13)	0.31 (15)
Cl(3)	−0.0267 (3)	0.4656 (6)	0.2408 (4)	4.95 (19)	4.56 (21)	9.89 (29)	0.92 (18)	0.95 (19)	−0.29 (23)
Cl(4)	0.0267 (3)	0.0884 (6)	0.0955 (3)	7.02 (22)	6.68 (28)	5.85 (22)	2.40 (22)	−3.10 (18)	−2.74 (22)

atom	x	y	z	B, Å^2	atom	x	y	z	B, Å^2
N(1)	0.1271 (8)	0.7509 (19)	0.1255 (9)	5.1 (2)	N(2)	0.1162 (8)	0.3995 (15)	0.5759 (9)	4.1 (2)
C(1)	0.1712 (9)	0.7572 (22)	0.2418 (10)	4.3 (3)	C(21)	0.1748 (10)	0.3729 (19)	0.6863 (12)	4.6 (3)
C(2)	0.2619 (9)	0.8596 (17)	0.2575 (11)	3.9 (3)	C(22)	0.2106 (10)	0.5288 (20)	0.7432 (12)	4.6 (3)
C(3)	0.3417 (8)	0.8132 (16)	0.1838 (10)	3.0 (2)	C(23)	0.2717 (9)	0.6253 (17)	0.6677 (10)	3.6 (3)
C(4)	0.2914 (9)	0.8104 (16)	0.0639 (10)	3.5 (3)	C(24)	0.2109 (10)	0.6525 (18)	0.5544 (11)	4.0 (3)
C(5)	0.2015 (10)	0.7063 (18)	0.0472 (12)	4.6 (3)	C(25)	0.1739 (10)	0.4921 (20)	0.5038 (12)	4.9 (3)
C(6)	0.4317 (9)	0.9231 (17)	0.2026 (11)	3.9 (3)	C(26)	0.3030 (10)	0.7836 (18)	0.7239 (11)	4.6 (3)
C(7)	0.5160 (9)	0.8730 (17)	0.1409 (10)	3.4 (2)	C(27)	0.3666 (8)	0.8863 (17)	0.6595 (10)	3.2 (2)
C(8)	0.5783 (8)	0.7480 (20)	0.1792 (9)	3.4 (2)	C(28)	0.4707 (10)	0.8778 (18)	0.6739 (11)	4.2 (3)
C(9)	0.6559 (9)	0.6951 (17)	0.1227 (11)	4.1 (3)	C(29)	0.5264 (9)	0.9715 (19)	0.6142 (11)	4.0 (3)
C(10)	0.6709 (9)	0.7711 (18)	0.0250 (10)	3.8 (3)	C(30)	0.4815 (11)	1.0780 (20)	0.5337 (11)	4.9 (3)
C(11)	0.6095 (9)	0.8910 (18)	−0.0154 (10)	3.8 (3)	C(31)	0.3793 (11)	1.0852 (20)	0.5194 (11)	4.9 (3)
C(12)	0.5327 (10)	0.9437 (18)	0.0406 (11)	4.3 (3)	C(32)	0.3219 (10)	0.9906 (19)	0.5799 (11)	4.2 (3)
H(1)[c]	0.0988	0.8579	0.1037	6.1	H(3)	0.0535	0.4587	0.5855	5.1
H(2)	0.0721	0.6703	0.1178	6.1	H(4)	0.0984	0.2943	0.5404	5.1
H(11)	0.1206	0.8008	0.2869	5.3	H(211)	0.1317	0.3155	0.7343	5.6
H(12)	0.1903	0.6471	0.2675	5.3	H(212)	0.2346	0.3063	0.6768	5.6
H(21)	0.2409	0.9718	0.2400	4.9	H(221)	0.1512	0.5924	0.7585	5.6
H(22)	0.2925	0.8522	0.3368	4.9	H(222)	0.2536	0.5046	0.8146	5.6
H(30)	0.3650	0.7031	0.2044	4.0	H(230)	0.3334	0.5640	0.6574	4.6
H(41)	0.2706	0.9211	0.0416	4.5	H(241)	0.1520	0.7216	0.5629	5.0
H(42)	0.3409	0.7711	0.0157	4.5	H(242)	0.2539	0.7057	0.5043	5.0
H(51)	0.1686	0.7175	−0.0310	5.6	H(251)	0.1304	0.5128	0.4322	5.9
H(52)	0.2229	0.5935	0.0612	5.6	H(252)	0.2335	0.4281	0.4895	5.9
H(61)	0.4100	1.0323	0.1777	4.9	H(261)	0.2410	0.8441	0.7342	5.6
H(62)	0.4568	0.9248	0.2837	4.9	H(262)	0.3419	0.7604	0.7979	5.6
H(80)	0.5673	0.6939	0.2498	4.4	H(280)	0.5053	0.8014	0.7291	5.2
H(90)	0.6996	0.6045	0.1520	5.1	H(290)	0.6011	0.9644	0.6281	5.0
H(100)	0.7272	0.7373	−0.0157	4.8	H(300)	0.5224	1.1453	0.4889	5.9
H(110)	0.6198	0.9424	−0.0872	4.8	H(310)	0.3449	1.1610	0.4637	5.9
H(120)	0.4887	1.0329	0.0094	5.3	H(320)	0.2472	0.9978	0.5659	5.2

[a] The anisotropic thermal parameter is defined by $\exp[-^1/_4(B_{11}h^2a^{*2} + B_{22}k^2b^{*2} + B_{33}l^2c^{*2} + 2B_{12}hka^*b^* + 2B_{13}hla^*c^* + 2B_{23}klb^*c^*)]$. [b] Esd's, shown in parentheses, are right adjusted to the least significant digit of the preceding number. They are derived from the inverse of the final least-squares matrix. [c] Hydrogen atoms were included at calculated positions, assuming a bond length of 1.0 Å, but neither coordinates nor thermal parameters (1.0 Å^2 greater than the bonded atom) were refined.

Table III. Interatomic Distances and Esd's (Å) for (4-BzpipdH)$_2$CoCl$_4$

(a) Distances within CoCl$_4{}^{2-}$ Anion

Co–Cl(1)	2.256 (4)	Cl(1)···Cl(3)	3.736 (5)
Co–Cl(2)	2.313 (4)	Cl(1)···Cl(4)	3.720 (6)
Co–Cl(3)	2.284 (5)	Cl(2)···Cl(3)	3.760 (7)
Co–Cl(4)	2.254 (4)	Cl(2)···Cl(4)	3.722 (5)
Cl(1)···Cl(2)	3.612 (5)	Cl(3)···Cl(4)	3.749 (6)

(b) Distances within 4-BzpipdH$^+$ Cations

N(1)–C(1)	1.46 (2)	N(2)–C(21)	1.48 (2)
N(1)–C(5)	1.52 (2)	N(2)–C(25)	1.47 (2)
C(1)–C(2)	1.49 (2)	C(21)–C(22)	1.53 (2)
C(2)–C(3)	1.54 (2)	C(22)–C(23)	1.54 (2)
C(3)–C(4)	1.53 (2)	C(23)–C(24)	1.53 (2)
C(3)–C(6)	1.52 (2)	C(23)–C(26)	1.53 (2)
C(4)–C(5)	1.49 (2)	C(24)–C(25)	1.54 (2)
C(6)–C(7)	1.50 (2)	C(26)–C(27)	1.51 (2)
C(7)–C(8)	1.39 (2)	C(27)–C(28)	1.39 (2)
C(7)–C(12)	1.40 (2)	C(27)–C(32)	1.38 (2)
C(8)–C(9)	1.40 (2)	C(28)–C(29)	1.36 (2)
C(9)–C(10)	1.39 (2)	C(29)–C(30)	1.40 (2)
C(10)–C(11)	1.36 (2)	C(30)–C(31)	1.37 (2)
C(11)–C(12)	1.39 (2)	C(31)–C(32)	1.39 (2)

Table IV. Bond Angles and Esd's (deg) for the (4-BzpipdH)$_2$CoCl$_4$

(a) Angles within CoCl$_4{}^{2-}$ Anion

Cl(1)–Co–Cl(2)	104.5 (1)	Cl(2)–Co–Cl(3)	109.7 (1)
Cl(1)–Co–Cl(3)	110.7 (1)	Cl(2)–Co–Cl(4)	109.1 (1)
Cl(1)–Co–Cl(4)	111.2 (1)	Cl(3)–Co–Cl(4)	111.4 (1)

(b) Angles within 4-BzpipdH$^+$ Cations

C(5)–N(1)–C(1)	113.5 (5)	C(25)–N(2)–C(21)	111.1 (6)
N(1)–C(1)–C(2)	111.6 (6)	N(2)–C(21)–C(22)	112.3 (6)
C(1)–C(2)–C(3)	113.8 (5)	C(21)–C(22)–C(23)	110.0 (5)
C(2)–C(3)–C(4)	107.7 (4)	C(22)–C(23)–C(24)	110.6 (5)
C(3)–C(4)–C(5)	113.1 (6)	C(23)–C(24)–C(25)	109.7 (6)
C(4)–C(5)–N(1)	111.1 (5)	C(24)–C(25)–N(2)	113.3 (5)
C(2)–C(3)–C(6)	111.3 (5)	C(22)–C(23)–C(26)	109.2 (5)
C(4)–C(3)–C(6)	113.6 (5)	C(24)–C(23)–C(26)	110.9 (5)
C(3)–C(6)–C(7)	113.2 (5)	C(23)–C(26)–C(27)	114.1 (5)
C(6)–C(7)–C(8)	120.6 (7)	C(26)–C(27)–C(28)	122.5 (7)
C(6)–C(7)–C(12)	122.3 (7)	C(26)–C(27)–C(32)	120.1 (7)
C(12)–C(7)–C(8)	117.1 (6)	C(32)–C(27)–C(28)	117.3 (6)
C(7)–C(8)–C(9)	122.3 (6)	C(27)–C(28)–C(29)	121.3 (7)
C(8)–C(9)–C(10)	118.5 (6)	C(28)–C(29)–C(30)	121.7 (7)
C(9)–C(10)–C(11)	120.2 (7)	C(29)–C(30)–C(31)	116.8 (7)
C(10)–C(11)–C(12)	121.3 (6)	C(30)–C(31)–C(32)	122.0 (7)
C(11)–C(12)–C(7)	120.5 (6)	C(31)–C(32)–C(27)	120.9 (7)

distortion according to the Muetterties and Guggenberger method,[15] since the two δ' angles of 108.2 and 108.7° (defined as the angles formed by the normals of the pair of triangular faces, which become a square face in the square-planar limit) are very close to the value of 109.5° for a regular tetrahedron. The other four δ angles range from 108.9 to 112.0°. Among

the factors which determine the deviation from T_d symmetry, we may include, as the most important one, the presence of one short hydrogen bond to Cl(4) and of two short hydrogen bonds to Cl(2) (Table VI), whose distance from Co (2.313 Å) is very close to the value of 2.306 Å found in (enH$_2$)$_2$-

Table V. Range of Bond Distances (Å) and Bond Angles (deg) and the Shape-Determining Dihedral Angles in Several $CoCl_4^{2-}$ Ions

	Co–Cl	Cl–Co–Cl	δ' angles
$Cs_2(CoCl_4)^a$	2.23	107.3–116.1	105.8, 108.5
$Cs_3(CoCl_4)Cl^b$	2.252	106.2–111.2	107.8, 107.8
$[N(CH_3)_4]_2(CoCl_4)^c$	2.229–2.266	108.3–112.8	106.8, 107.4
$(HistH_2)(CoCl_4)^d$	2.233–2.295	105.7–115.3	105.3, 105.6
$(C_{13}H_{19}N_2OS)_2(CoCl_4)^e$	2.230–2.317	105.1–111.7	107.1, 107.8
$(enH_2)_2(CoCl_4)Cl_2^f$	2.265–2.306	103.3–126.3	98.9, 103.6
$(4\text{-BzpipdH})_2(CoCl_4)$	2.254–2.313	104.5–111.4	108.2, 108.7

^{a} Reference 9. ^{b} Reference 10. ^{c} Reference 11. ^{d} Reference 12. ^{e} Reference 13. ^{f} Reference 14.

Table VI. Hydrogen-Bonding Distances (Å) and Angles (deg) for $(4\text{-BzpipdH})_2CoCl_4$

atoms	Cl···N	Cl···H	Cl···H–N
$Cl(2)\cdots H(4)–N(2)$	3.222	2.275	157.5
$Cl(2)\cdots H(3^{III})–N(2^{III})^a$	3.177	2.181	173.8
$Cl(4)\cdots H(1^{II})–N(1^{II})$	3.147	2.166	166.4

^{a} The superscript refers to the symmetry transformation of Figure 3.

$(CoCl_4)Cl_2^{13}$ and of 2.317 Å in $(C_{13}H_{19}N_2OS)_2(CoCl_4)^{14}$ for Cl atoms similarly engaged in hydrogen bonding.

Of the two crystallographically independent $(4\text{-BzpipdH})^+$ ions the piperidine rings are both chair shaped with torsion angles ranging, as absolute values, from 52.3 to 54.5° for cation 1 and from 54.5 to 56.2° for cation 2 (by assigning to cations the numbering of the N atom that they include). Bond lengths and angles are within expected values, with the exception of some distances in the piperidine ring of cation 1 (one anomalously long C–N bond distance of 1.52 Å and two short C–C bond lengths of 1.49 Å). Both the benzyl groups are bonded to the piperidine ring in equatorial positions; for cation

1 the dihedral angle between the least-squares plane of the phenyl ring and that defined by the C(1), C(2), C(4), and C(5) atoms is 86.3°, the corresponding angle on cation 2 being 75.5° (the maximum deviation of an atom from the plane is 0.010 Å on phenyl ring 1).

Hydrogen bondings are the most notable feature differentiating the cations. While in cation 1 there is a single hydrogen bond between the equatorial hydrogen of N(1) and the Cl(4) atoms, cation 2 acts, by means of the two hydrogen atoms bonded to N(2), as a bridge between two symmetry-related Cl(2) atoms, linking the anions into infinite chains, running parallel to the *b* axis, which determine the crystal packing (Figure 3 and Table VI). These chains are separated by normal van der Waals distances.

Magnetic Moments and Electronic, X-ray Powder, and Far-IR Spectra. The corrected room-temperature magnetic moments (Table VIII) are most easily interpreted on the assumption that all the compounds are essentially tetrahedral. A gradual increase in the value of magnetic moments, observed when more a polarizable halide ion is introduced into the coordination sphere, is probably due to the increasing orbital contribution to the singlet ground state on passing from chlorine to iodine.[16]

Although the shape of the electronic spectra of the complexes suggests distortion from tetrahedral symmetry, the envelope of the d–d bands does not permit accurate band assignments in the reduced symmetry. Therefore the electronic spectra are interpreted and assigned (as reported in Table VII) on the basis of simple ligand field considerations for a d^7 ion in a tetrahedral field. The $^4A_2(F) \rightarrow {}^4T_2(F)$ (ν_1) band is not observed as it occurs at low energy[17] and may be obscured by vibrational transitions of the cations.

The ligand field parameters (Table VIII), calculated from the gravity center of the ν_2 and ν_3 bands, are in fair agreement with other reported values for tetrahedral CoX_4^{2-} ions.[18]

Table VII. Room-Temperature Electronic Spectra (nm) of the Tetrahalocobaltates(II) in the Solid State

	d–d bands		spin-forbidden and charge-transfer bands
	$^4A_2(F) \rightarrow {}^4T_1(F)$ (ν_2)	$^4A_2(F) \rightarrow {}^4T_1(P)$ (ν_3)	
$(N\text{-EtpipdH})_2CoCl_4$	2190 sh, 2045 sh, 1825, 1660	697, 665, 643 sh, 632, 618 sh	575 sh, 565 sh, 550, 532, 508 sh, 492 sh, 465 sh, 450, 416, 408, 380
$(N\text{-EtpipdH})_2CoBr_4$	2300, 2100, 1965, 1815	730, 702, 668, 657 sh, 645, 630 sh	605, 593, 582, 569, 540 sh, 525 sh, 485, 475, 467, 462 sh, 438, 430, 400
$(N\text{-EtpipdH})_2CoI_4$	2500 sh, 2280, 2000 sh	785, 760 sh, 730, 701	631, 602, 572 sh, 555, 525 sh, 515 sh, 500 sh, 480 sh, 453 sh, 380
$(2\text{-EtpipdH})_3(CoCl_4)Cl$	2135 sh, 1965 sh, 1830, 1640	682, 665, 640, 631, 612 sh	575 sh, 500, 532, 507 sh, 490 sh, 450, 416, 408, 380
$(2\text{-EtpipdH})_2CoBr_4$	2250 sh, 1955, 1780	725, 698, 665, 650 sh, 641	606, 590, 580, 568, 552, 535 sh, 518 sh, 482, 471, 463, 456 sh, 432, 425, 395, 375 sh
$(2\text{-EtpipdH})_2CoI_4$	2400 sh, 2180, 2000	782, 750 sh, 727, 697	635, 600 sh, 582 sh, 550, 521, 510 sh, 498, 484 sh, 472, 460 sh, 420 sh, 380
$(4\text{-BzpipdH})_2CoCl_4$	2105, 1940 sh, 1830, 1650	615 sh, 628, 645 sh, 672, 705	564 sh, 550, 534, 504 sh, 488 sh, 472, 450, 408
$(4\text{-BzpipdH})_2CoBr_4$	2290, 2115, 1975, 1810	651, 675, 710, 740	610, 597 sh, 582, 570, 539, 525 sh, 487, 475, 469, 461 sh, 437, 430, 398
$(4\text{-BzpipdH})_2CoI_4$	2350 sh, 2025	710, 740, 770 sh, 798	645, 615, 586, 558, 530, 516 sh, 505, 480, 465 sh, 395

Table VIII. Spectral and Magnetic Data and Derived Electronic Structure Parameters for the Complexes

	ν_2, cm^{-1}	ν_3, cm^{-1}	Dq, cm^{-1}	B', cm^{-1}	β $(B'/B_0)^a$	TIP, cgsu × 10^{-6}	μ_{cor}, μ_B
$(N\text{-EtpipdH})_2CoCl_4$	5405	14 880	309	733	0.75	676	4.76
$(N\text{-EtpipdH})_2CoBr_4$	4880	14 090	279	707	0.73	749	4.82
$(N\text{-EtpipdH})_2CoI_4$	4500	12 900	257	646	0.67	813	4.87
$(2\text{-EtpipdH})_3(CoCl_4)Cl$	5430	14 860	311	731	0.75	672	4.84
$(2\text{-EtpipdH})_3CoBr_4$	5000	14 330	286	719	0.74	730	4.91
$(2\text{-EtpipdH})_2CoI_4$	4670	12 900	267	637	0.66	783	4.64^b
$(4\text{-BzpipdH})_2CoCl_4$	5430	14 710	311	720	0.74	672	4.65
$(4\text{-BzpipdH})_2CoBr_4$	4930	13 790	282	684	0.70	741	4.83
$(4\text{-BzpipdH})_2CoI_4$	4610	12 770	264	631	0.65	792	4.88

^{a} B(free ion) = 971 cm^{-1}. ^{b} This value is only indicative since the compound is strongly hygroscopic and difficult to handle.
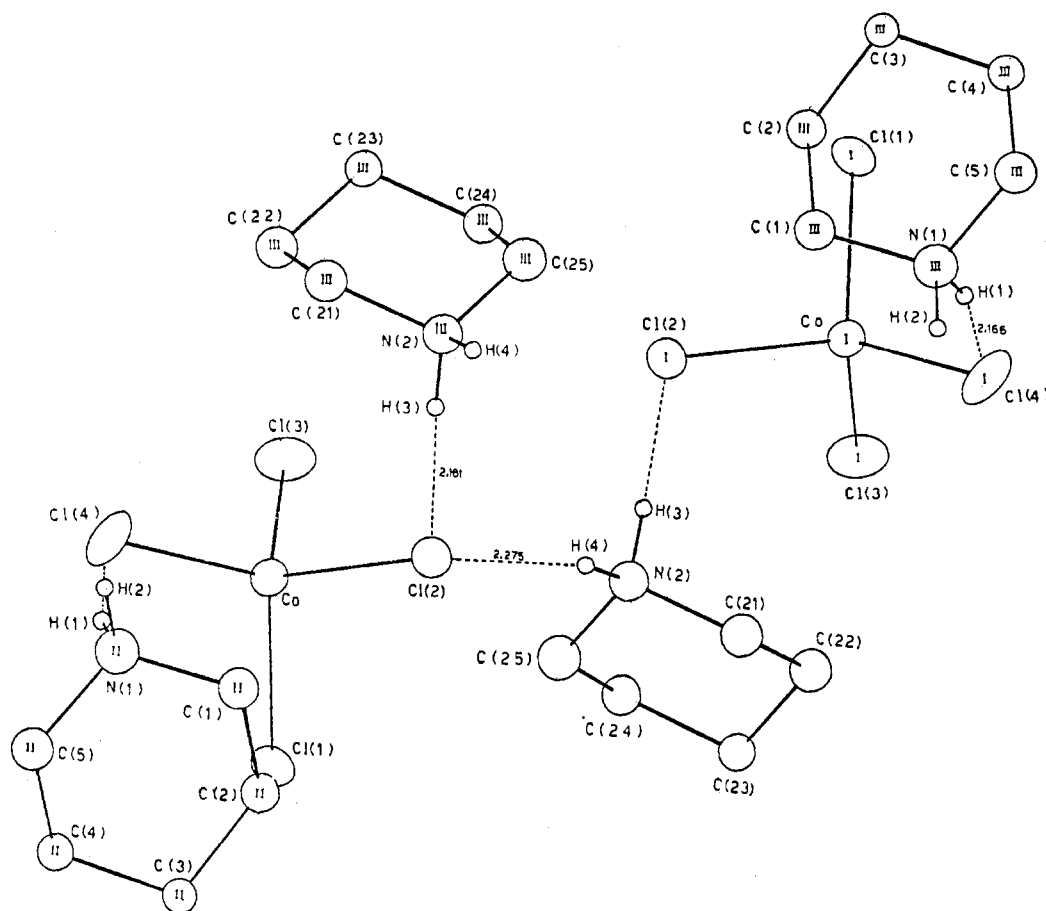
Figure 3. Hydrogen bonds (dashed lines) in (4-BzpipdH)$_2$CoCl$_4$. The projection is along the *b* axis; benzyl groups and C-bonded hydrogen atoms have been omitted for clarity. Roman numerals on atoms refer to the following symmetry transformations: I, $-x$, $^1/_2 + y$, $1 - z$; II, x, $1 - y$, z; III, $-x$, $y - ^1/_2$, $1 - z$.
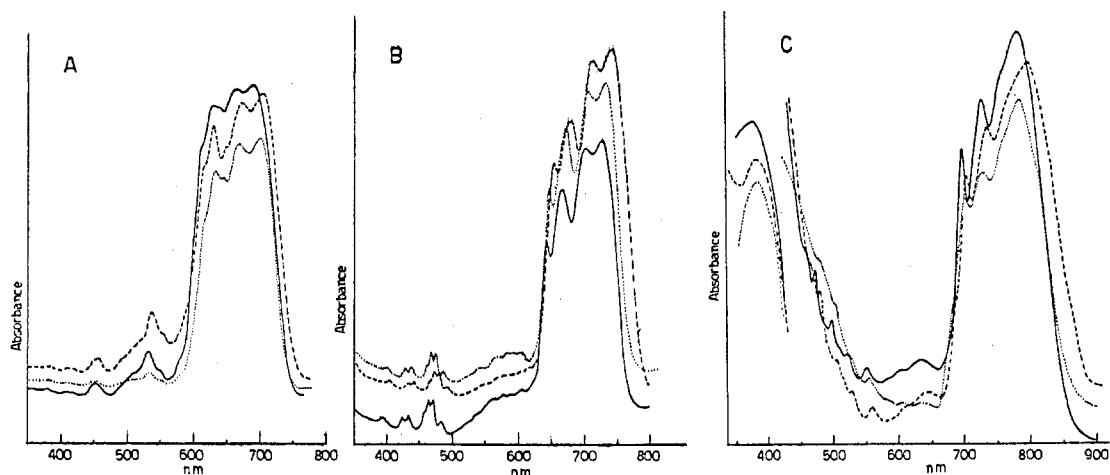

Figure 4. Solid-state electronic spectra of (*N*-EtpipdH)$_2$CoX$_4$ (···), (2-EtpipdH)$_2$CoX$_4$ (—), and (4-BzpipdH)$_2$CoX$_4$ (---) (X = Cl (A), Br (B), I (C)).

Figure 4 reports the strong absorption bands of the complexes, appearing in the 810–610-nm spectral range, assignable to the $^4A_2 \rightarrow {}^4T_1(P)$ transition,[5,19] which show a considerable fine structure. As the bandwidth of the 4-BzpipdH complexes is larger than that of the other complexes, a distortion of the former greater than that of the latter may be suggested.[14]

The X-ray powder spectra show that none of the compounds are isomorphous.

The far-IR spectra of the hydrohalide salts and the complexes are given in Table IX. The metal–halogen stretching vibrations are assigned with reasonable certainty, since several sets of compounds of the same stereochemistry are available

in which the halogens are varied from Cl to Br to I.

The metal–halogen vibrations of all the complexes, except that of the crystallographically known (4-BzpipdH)$_2$CoCl$_4$ complex, may be assigned on the basis of tetrahedral or distorted tetrahedral symmetry in agreement with values quoted for tetrahedral tetrahalocobaltates(II).[20-23] Observed splitting of the fundamental IR-active (M–X) vibrations may be attributed to distortion or crystal effects.[21,24]

For the (4-BzpipdH)$_2$CoCl$_4$ complex the point group is C_2. This arrangement would allow four metal–halogen stretching modes. In fact the $v_1(A_1)$ and $v_3(F_2)$ bands in T_d symmetry respectively give rise to one (A) and three (A + B + B)

Table IX. Far-Infrared Spectra (cm^{-1}) of the Hydrohalide Salts and the Complexes in the Solid State

	ν(CoX)	other bands below 400 cm^{-1}
N-EtpipdHI		374 m, 337 w, 152 ms, 113 s, 77 m, b
(*N*-EtpipdH)$_2$CoCl$_4$	313 sh, 290 vs, b, 266 sh	374 m, 162 sh, 153 ms, 130 sh, 86 m
(*N*-EtpipdH)$_2$CoBr$_4$	232 s, 218 s	372 w, 340 vw, 150 vw, 112 s, b, 70 w
(*N*-EtpipdH)$_2$CoI$_4$	195 s, 186 vs	372 w, 340 w, 100 s, b, 54 vw
2-EtpipdHCl		375 m, 342 w, 284 vs, 228 w, 179 vs, 154 s, 138 sh, 94 m
2-EtpipdHBr		370 m, 340 w, 274 s, 261 s, 226 w, 159 m, b, 104 s, b
2-EtpipdHI		367 s, 336 m, 249 vs, 155 vs, 120 m, 84 s
(2-EtpipdH)$_3$(CoCl$_4$)Cl	302 vs, b, 288 sh	374 m, 340 sh, 251 m, 226 sh, 174 sh, 155 ms, 138 ms, 92 m
(2-EtpipdH)$_2$CoBr$_4$	234 s, b, 220 sh	372 m, 340 vw, 250 sh, 150 m, 106 ms, 98 m, 70 w
(2-EtpipdH)$_2$CoI$_4$	197 s, b, 188 sh	375 vw, 334 vw, 252 m, 226 vw, 158 w, 152 sh, 98 s, b, 86 sh, 57 m
4-BzpipdHCl		340 w, 276 w, 243 w, 223 m, 210 ms, 150 ms, 139 sh, 100 m
4-BzpipdHBr		345 w, 333 w, 269 w, 240 w, 219 w, 190 m, b, 124 m, 100 w, 76 w
4-BzpipdHI		325 w, 268 w, 244 w, 221 m, 176 w, 99 w
(4-BzpipdH)$_2$CoCl$_4$	320 s, 300 vs, 280 s, 251 s	360 w, 330 sh, 270 sh, 228 w, 190 ms, 159 ms, 149 sh, 122 m, 100 w
(4-BzpipdH)$_2$CoBr$_4$	237 vs, 222 s	354 w, 320 mw, 279 mw, 170 m, 128 ms, 88 m
(4-BzpipdH)$_2$CoI$_4$	204 s, 192 m	352 w, 319 mw, 267 mw, 223 sh, 168 mw, 112 m, 76 vw
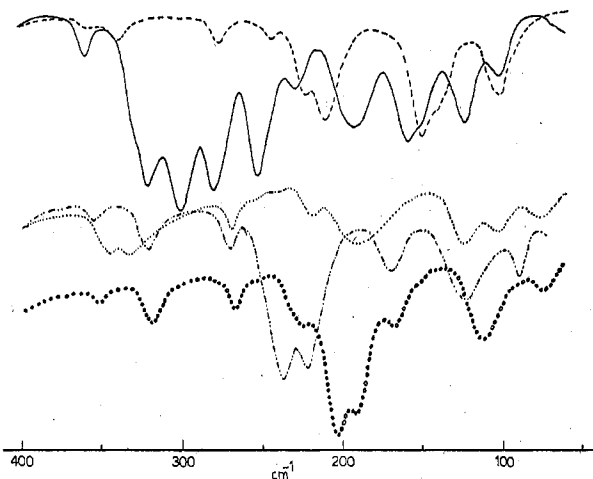
Figure 5. Solid-state far-infrared spectra of 4-BzpipdHCl (- - -), (4-BzpipdH)$_2$CoCl$_4$ (—), 4-BzpipdHBr (···), (4-BzpipdH)$_2$CoBr$_4$ (-····-), and (4-BzpipdH)$_2$CoI$_4$ (OOO) compounds.

vibrations, IR and Raman active, in C_2 symmetry. The four experimental bands appearing in the far-IR spectra of the (4-BzpipdH)$_2$CoCl$_4$ complex, by comparison with the spectra of the hydrohalide salts, of the other (4-BzpipdH)$_2$CoX$_4$ (X = Br, I) complexes (Figure 5), and of other chlorometalates (M = Cu, Sb) of the same cation,[25] may be reasonably assigned to the metal–chlorine stretching vibrations and in particular those having lower intensity (320 (s) and 251 (s) cm^{-1}) to the A modes and those having higher intensity (300 (vs) and 280 (s) cm^{-1}) to the B modes.

Hydrogen Bonding. Evidence for the presence of hydrogen bonds in the complexes may also be found by comparing their IR spectra with those of the hydrohalide salts. In fact the bands assignable to the NH motions in the cations, which are found at 2900–2700 cm^{-1} (ν(NH$_2^+$)) in the 2-EtpipdH and 4-BzpipdH cations and at 2700–2600 cm^{-1} (ν(NH$^+$)) in the *N*-EtpipdH cation,[26,27] are shifted to higher energies (3200–3000 cm^{-1}) in the complexes. As these bands in the (4-BzpipdH)$_2$CoX$_4$ complexes are shifted to higher energies (3190–65 and 3140–20 cm^{-1}) than in the other complexes (3040–10 cm^{-1}), the presence of hydrogen bonding interactions in the former being stronger than in the latter complexes may be suggested.

For a reasonable explanation of a tetrahedral distortion of the 4-BzpipdH complexes greater than that of the *N*-EtpipdH and 2-EtpipdH complexes, we should consider not only the hydrogen-bonding ability of the cations, those of the 2-EtpipdH and 4-BzpipdH cations being practically identical, but also the effect of the cation dimensions in the crystal packing of the molecules, which for the 4-BzpipdH cation is much greater

than that for the other cations considered in this work.

References and Notes

(1) (a) Istituto di Chimica Generale e Inorganica, University of Modena, 41100 Modena, Italy. (b) Istituto di Chimica, Facoltà di Medicina-Veterinaria, University of Bari, 70126 Bari, Italy.
(2) Marcotrigiano, G.; Menabue, L.; Pellacani, G. C. *Inorg. Chem.* **1976**, *15*, 2333.
(3) Battaglia, L. P.; Bonamartini Corradi, A.; Marcotrigiano, G.; Menabue, L.; Pellacani, G. C. *Inorg. Chem.* **1979**, *18*, 148.
(4) Cariati, F.; Marcotrigiano, G.; Menabue, L.; Morazzoni, F.; Pellacani, G. C.; Zanderighi, G. M. *Spectrochim. Acta, Part A* **1978**, *34*, 801.
(5) Cotton, F. A.; Goodgame, D. M. L.; Goodgame, M. *J. Am. Chem. Soc.* **1961**, *83*, 4690.
(6) "User Manual for PW1100 Philips"; Philips: Eindhoven.
(7) Cromer, D. T.; Waber, J. T. "International Tables of X-Ray Crystallography"; Kynoch Press: Birmingham, England, 1974; Vol. IV.
(8) All the calculations were carried out on a Cyber 7600 computer of the Centro di Calcolo Interuniversitario dell'Italia Nord Orientale, Bologna, using a set of programs written by A. Immirzi, which includes least-squares program MIQUAD [*Ric. Sci.* **1967**, *37*, 743] and Fourier program FFSYNT [*J. Appl. Crystallogr.* **1973**, *6*, 246]. Johnson's ORTEP thermal ellipsoid plotting programs were used for drawing.
(9) Porai-Koshits, M. A. *Tr. Inst. Kristallogr., Akad. Nauk SSSR* **1954**, No. 10, 117.
(10) Figgis, B. N.; Gerloch, M.; Mason, R. *Acta Crystallogr., Sect. B* **1964**, *17*, 506.
(11) Wiesner, J. R.; Srivastana, R. C.; Kennard, C. H. L.; DiVaira, M.; Lingafelter, E. C. *Acta Crystallogr., Sect. B* **1967**, *23*, 565.
(12) Bonnet, J. J.; Jeannin, Y. *Acta Crystallogr., Sect. B* **1972**, *28*, 1079.
(13) Bonamartini Corradi, A.; Nardelli, M.; Palmieri, C. *Acta Crystallogr., Sect. B* **1972**, *28*, 1207.
(14) Smith, H. W.; Stratton, W. J. *Inorg. Chem.* **1977**, *16*, 1640.
(15) Muetterties, E. L.; Guggenberger, L. J. *J. Am. Chem. Soc.* **1974**, *96*, 1748.
(16) Jha, N. K.; Saxena, A. *Inorg. Chim. Acta* **1978**, *26*, 201.
(17) Quinn, M. B.; Smith, D. W. *J. Chem. Soc. A* **1971**, 2496.
(18) Fogel, N.; Lin, C. C.; Ford, C.; Grindstaff, W. *Inorg. Chem.* **1964**, *3*, 720.
(19) Ferguson, J. *J. Chem. Phys.* **1963**, *39*, 116.
(20) Sabatini, A.; Sacconi, L. *J. Am. Chem. Soc.* **1964**, *86*, 17.

(21) Dunsmuir, J. T. R.; Lane, A. P. *J. Chem. Soc. A* **1974**, 404.
(22) Edwards, H. G. M.; Woodward, L. A.; Gall, M. J.; Ware, M. J. *Spectrochim. Acta, Sect. A* **1970**, *26* 287.
(23) Ferraro, J. R. *J. Coord. Chem.* **1976**, *5*, 101.
(24) Clark, R. J.; Dunn, T. M. *J. Chem. Soc. A* **1963**, 1198.
(25) Work in progress.
(26) Colthrum, N. B.; Daly, L. H.; Wiberley, S. E. "Introduction to Infrared and Raman Spectroscopy"; Academic Press: New York, 1975; p 282.
(27) Bellamy, L. J. "The Infrared Spectra of Complex Molecules"; Chapman and Hall: London, 1975; pp 267, 290.

Contribution from the Research School of Chemistry,
Australian National University, Canberra, A.C.T., Australia 2600

Metal Complexes of Hemilabile Ligands. Reactivity and Structure of Dichlorobis(*o*-(diphenylphosphino)anisole)ruthenium(II)

JOHN C. JEFFREY*[1] and THOMAS B. RAUCHFUSS*[1]

The red complex $RuCl_2(PO)_2$ (**1**) (PO = *o*-(diphenylphosphino)anisole) crystallizes from dichloromethane/hexane as a solvate, $RuCl_2(PO)_2 \cdot CH_2Cl_2$, and has been characterized by a single-crystal X-ray structural analysis. The crystals have space group $P2_1/n$ with $a = 11.194$ (1) Å, $b = 28.294$ (4) Å, $c = 12.458$ (1) Å, $\beta = 95.50$ (1)°, $Z = 4$, $\rho_{obsd} = 1.40$ g/cm³, and $\rho_{calcd} = 1.40$ g/cm³. The complex is six-coordinate with trans chlorine and cis phosphorus donor atoms. The Ru–P distances of 2.217 (1) and 2.219 (1) Å, are similar to those found for apical phosphines in square-pyramidal ruthenium(II) complexes. The Ru–O distances of 2.299 (3) and 2.257 (3) Å are greater than that of the sum of the respective covalent radii, consistent with a weak Ru–O bond. **1** undergoes reversible electrochemical oxidation in acetone at 0.778 V vs. Ag/AgCl and chemical oxidation with $NOBF_4$ to afford the paramagnetic complex $[RuCl_2(PO)_2](BF_4)$ (**2**), characterized by its ESR spectrum. The room-temperature reaction of **1** with CO gives initially a fluxional monomeric complex, $RuCl_2(PO)_2(CO)$ (**4**), and then *all-trans*-$RuCl_2(PO)_2(CO)_2$ (**3**), via dissociation of the Ru–O bonds. Reaction of **1** with CO at elevated temperatures gives a new *cis*-dicarbonyl isomer, $RuCl_2(PO)_2(CO)_2$ (**5**), which has trans phosphines. Unlike **4**, complex **5** does not readily lose CO thermally; however, it is photochemically converted to a mixture of **3** and **4**. Closely related reactions are observed when **1** is treated with *tert*-butyl isocyanide and the species $RuCl_2(PO)_2(t\text{-BuNC})_2$ (**6**) and $RuCl_2(PO)_2(t\text{-BuNC})$ (**7**) were identified spectroscopically (and isolated for **6**). A reaction scheme rationalizing the formation of **3**, **4**, **5**, **6**, and **7** is presented and the results are discussed in light of the known work on phosphinoanisole–transition-metal complexes.

Introduction

Studies of the coordination chemistry of transition metal phosphines are useful in understanding the catalytic activity of this class of compounds. The majority of the catalytically useful group 8 metal ions contain triphenylphosphine, e.g., $RhCl(PPh_3)_3$, $Rh(H)CO(PPh_3)_3$, $RuHCl(PPh_3)_3$, and $Ru(H)(O_2CCH_3)(PPh_3)_3$.[2] This is largely a matter of convenience, other phosphines being air sensitive, expensive, or not available commercially. In the past few years, however, more complex phosphines have been found in many applications to be superior to triphenylphosphine. This is especially true in the area of asymmetric hydrogenation and hydrosilylation.[3-6]

For some time, we have investigated the chemistry of phosphine–amine and phosphine–ether ligands with the expectation that these ligands would bind well enough to allow isolation but would readily dissociate the "hard" ligand component, thus generating a vacant site for substrate binding.[7] We call these ligands *hemilabile*.

The ruthenium chelates derived from *o*-(diphenylphosphino)anisole, PO, are precursors to active hydrogenation and

PO
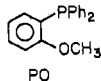
isomerization catalysts and are related to the well-known Monsanto asymmetric catalysts, since both systems utilize phosphine–ether ligands. In a series of papers Shaw and co-workers have described the chemistry of other platinum metal complexes of phosphine anisoles.[9]

Experimental Section

All compounds described herein are air stable, both as solutions and in the solid state; nonetheless, reactions were performed in an inert atmosphere. Compounds were routinely recrystallized from dichloromethane; however, as it is often difficult to completely remove or stoichiometrically retain solvent in the crystalline solids obtained

from it, the analyses are often only fair. Molecular weights were measured by vapor pressure osmometry in CH_2Cl_2. The electrochemical experiment was performed on apparatus described elsewhere.[11]

Improved Preparation of $RuCl_2(PO)_2$ (1). A 11.5-g sample of PO[12] (PO = *o*-(diphenylphosphino)anisole) was dissolved in 500 mL of boiling EtOH. A 4.5-g sample of Engelhardt "ruthenium trichloride" (35% Ru) was dissolved in 5 mL of H_2O in a steam bath and diluted with 10 mL of EtOH. The ruthenium solution was rapidly added to the phosphine solution at reflux and the brown mixture was boiled. After 30 min the solution was deep red and was allowed to cool overnight. The red crystals were filtered and washed with 100 mL of EtOH and 200 mL of Et_2O; yield 9.0 g.

Anal. Calcd for $C_{38}H_{34}Cl_2O_2P_2Ru$: C, 60.21; H, 4.50; Cl, 9.38; P, 8.20. Found: C, 60.6; H, 4.78; Cl, 9.36; P, 8.41.

$[RuCl_2(PO)_2]BF_4 \cdot CH_2Cl_2$ (2). A 187-mg sample of $Ru(PO)_2Cl_2$ (0.25 mmol) was suspended in MeCN and 30 mg of $NOBF_4$ was quickly added. The red suspension dissolved to give a homogeneous dark red solution which was evaporated. Crystallization from CH_2Cl_2 by the addition of Et_2O gave the product as the CH_2Cl_2 solvate.

Anal. Calcd for $C_{39}H_{36}BCl_4F_4O_2P_2Ru$: C, 50.40; H, 3.88; Cl, 15.30; P, 6.7. Found: C, 50.44; H, 4.04; Cl, 16.27; N, 0.00; P, 6.86.

***trans,trans,trans*-$RuCl_2(PO)_2(CO)_2$ (3).** A 220-mg sample of $Ru(PO)_2(CO)_2Cl_2$ was dissolved in 10 mL of CH_2Cl_2. After thorough saturation with CO for ca. 0.5 h, hexane was added in small portions while the CO atmosphere was maintained. After the complex had been precipitated, it was filtered and recrystallized from CH_2Cl_2–hexane under a CO atmosphere.

Anal. Calcd for $C_{40}H_{34}Cl_2O_2P_2Ru$: C, 59.11; H, 4.18; Cl, 8.7; P, 7.6. Found: C, 59.27; H, 4.48; Cl, 9.55; P, 7.61.

$Ru(PO)_2(CO)Cl_2$ (4). Samples of this complex were prepared as described previously.[7] For NMR purposes, it was found easier to prepare it in situ from *trans*-$RuCl_2(PO)_2(CO)$ (3) by displacement of the carbon monoxide by an argon purge; mol wt calcd 800, found 819.

***cis,trans,cis*-$RuCl_2(PO)_2(CO)_2$ (5).** $Ru(PO)_2Cl_2$, 300 mg, was heated in 20 mL of decane from 95 to 135 °C during 10 h in an atmosphere of CO. After the reaction period, the almost colorless solid was filtered and washed with pentane. The cream solid was